

Low cost alternative of high speed visible light camera for tokamak experiments

T. Odstrcil, M. Odstrcil, O. Grover, V. Svoboda, I. Ďuran et al.

Citation: *Rev. Sci. Instrum.* **83**, 10E505 (2012); doi: 10.1063/1.4731003

View online: <http://dx.doi.org/10.1063/1.4731003>

View Table of Contents: <http://rsi.aip.org/resource/1/RSINAK/v83/i10>

Published by the [American Institute of Physics](#).

Related Articles

Ultra fast x-ray streak camera for ten inch manipulator based platforms

Rev. Sci. Instrum. **83**, 10E106 (2012)

X-ray bang-time measurements at the National Ignition Facility using a diamond detector

Rev. Sci. Instrum. **83**, 10E105 (2012)

Design and analysis of multi-color confocal microscopy with a wavelength scanning detector

Rev. Sci. Instrum. **83**, 053704 (2012)

Short wavelength thermography: Theoretical and experimental estimation of the optimal working wavelength

J. Appl. Phys. **111**, 084903 (2012)

Hole shape effect induced optical response to permittivity change in palladium sub-wavelength hole arrays upon hydrogen exposure

J. Appl. Phys. **111**, 084502 (2012)

Additional information on Rev. Sci. Instrum.

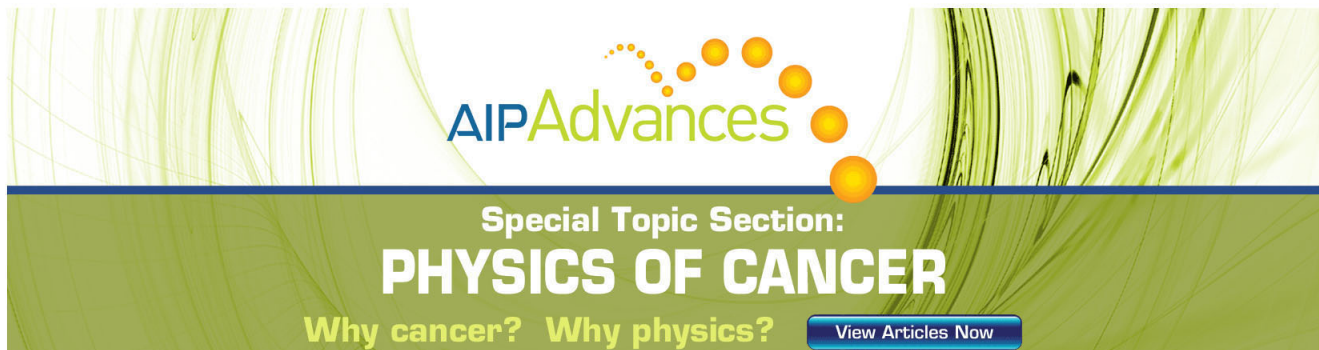
Journal Homepage: <http://rsi.aip.org>

Journal Information: http://rsi.aip.org/about/about_the_journal

Top downloads: http://rsi.aip.org/features/most_downloaded

Information for Authors: <http://rsi.aip.org/authors>

ADVERTISEMENT



AIPAdvances

Special Topic Section:
PHYSICS OF CANCER

Why cancer? Why physics? [View Articles Now](#)

Low cost alternative of high speed visible light camera for tokamak experiments^{a)}

T. Odstrcil,¹ M. Odstrcil,^{1,2} O. Grover,¹ V. Svoboda,^{1,b)} I. Ďuran,^{1,2} and J. Mlynář^{1,2}

¹Czech Technical University in Prague, FNSPE, Břehová 7, CZ-115 19 Praha 1, Czech Republic

²Institute of Plasma Physics AS CR, v.v.i., Association Euratom-IPP.CR, Za Slovankou 3, CZ-182 00 Praha 8, Czech Republic

(Presented 8 May 2012; received 6 May 2012; accepted 1 June 2012; published online 28 June 2012)

We present design, analysis, and performance evaluation of a new, low cost and high speed visible-light camera diagnostic system for tokamak experiments. The system is based on the camera Casio EX-F1, with the overall price of approximately a thousand USD. The achieved temporal resolution is up to 40 kHz. This new diagnostic was successfully implemented and tested at the university tokamak GOLEM ($R = 0.4$ m, $a = 0.085$ m, $B_T < 0.5$ T, $I_p < 4$ kA). One possible application of this new diagnostic at GOLEM is discussed in detail. This application is tomographic reconstruction for estimation of plasma position and emissivity. © 2012 American Institute of Physics. [<http://dx.doi.org/10.1063/1.4731003>]

I. INTRODUCTION

A high speed visible camera is a standard diagnostic tool for most magnetic confinement fusion experiments. These cameras serve a wide range of purposes¹ including measurement of emissivity profiles of hydrogen isotopes and certain impurities, visualization of transient events in the edge and scrape-off layer plasmas, passive imaging of visible bremsstrahlung, etc. Generally, a setup providing a high spatial resolution and a high frame rate of at least 1 kHz is required to address most of these tasks. Endurance in high magnetic fields and non-negligible radiation doses can be an issue for applications of such a diagnostic at certain fusion experiments. The relatively high price is one of the main disadvantages of the commercially available scientific solutions, possibly being even prohibitive when considering installation of such products at small, university-based plasma experiments. We present a new low cost solution, suitable for smaller tokamak experiments, based on the commercially available camera Casio Exilim EX-F1. We demonstrate performance of this camera for tomography.

II. EXPERIMENTAL SETUP

A. High speed camera Casio EX-F1

The Casio EX-F1 is a commercially available camera with high speed imaging capabilities. This camera is interesting especially because of its low price. It costs less than 1000 USD while any cheap scientific high speed camera costs more than 4000 USD and scientific cameras with comparable maximum frame rate, higher resolution, and dynamic range are even more expensive.

The camera is equipped with a zoom lens with an antireflexive coating. Entrance pupil size is $\phi 4.5$ cm, the field of view is variable from 9.2° to 88° with the corresponding maximal numerical aperture from 0.11 to 0.18.

The camera contains a CMOS imaging chip IMX017CGE (Ref. 2) with a maximum 6.2 megapixels resolution. The camera can operate in various regimes. We have used a high-speed (HS) movie mode that allows up to 1200 fps with a resolution of 336×96 pixels. Finally, it is possible to use the so-called rolling shutter effect³ to increase the time resolution even up to the effective 40 000 fps with a resolution of 336×1 pixels (successively 96 rows of the CMOS chip). The principle of the rolling shutter is shown in Fig. 1. Each pixel row from the CMOS sensor is read out separately by parallel readout circuits. The time shift of the electronic shutter in consecutive rows is given by the readout time. Furthermore, when the last row of CMOS chip is reached, there is a time lag equal to 17% of the frame time, which is needed for processing of each full image (see Fig. 1). Then, the readout cycle can begin again starting from the first row. Detailed timing is in Ref. 2.

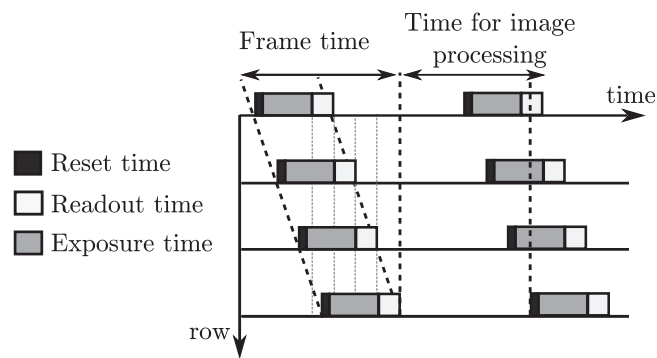


FIG. 1. A simplified example of timing of the image readout in rolling shutter mode for the case of CMOS chip. Each box corresponds to processing time of one row.

^{a)}Contributed paper, published as part of the Proceedings of the 19th Topical Conference on High-Temperature Plasma Diagnostics, Monterey, California, May 2012.

^{b)}Author to whom correspondence should be addressed. Electronic mail: svoboda@fjfi.cvut.cz.

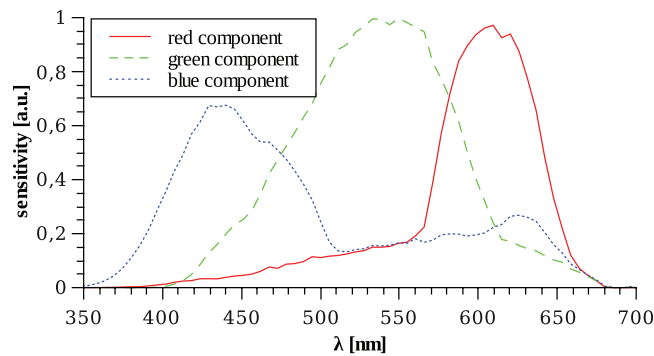


FIG. 2. Measured relative spectral sensitivity of the CMOS sensor and camera firmware color adjustment.

We measured the basic sensor parameters in order to correctly evaluate plasma emissivity. Signal from CMOS chip is read in 10-bit resolution, however, than it is nonlinearly quantized and stored to a compressed RGB format with only 8-bit per color resolution. According to our measurement, the correct linearization of the quantization function is well approximated by $y = x/(bx + a)$ where y is proportional to the normalized light intensity, x is the intensity stored in the image, and the constants are $a = 43000 \pm 600$, $b = 140 \pm 3$. This method preserved the maximal dynamic range 60 dB. The maximum length of a single record is limited to 440 s. The minimal exposure time is $25 \mu\text{s}$.

Finally, the spectral sensitivity of the CMOS sensor was measured (see normalized data in Fig. 2).

B. Arrangement of the fast visible camera diagnostic on GOLEM

Experiments were conducted at the small tokamak GOLEM (Ref. 4) ($R = 0.4$ m, $a = 0.085$ m, $B_T < 0.5$ T, $I_p < 4$ kA) located in Prague, Czech Republic. The typical length of a plasma discharge is 15 ms. One example of the application for tokamak plasma diagnostics was commissioned and evaluated: visible light tomography. The camera Casio EX-F1 was operated in rolling shutter regime.

Firstly, we performed a tomographic reconstruction of plasma emissivity. Tomographic reconstruction is generally an ill conditioned problem; therefore, it is necessary to observe the plasma column from many different lines of sight. In our case, two HS cameras were placed on perpendicular diagnostic ports as it is shown in Fig. 3. Orientation of the cameras was set so that the horizontal rows of the CMOS chip were rotated perpendicularly to the toroidal magnetic field direction in order to allow exploitation of the rolling shutter effect.

C. Image preprocessing

Before further analysis of the images taken by the HS camera they have to be significantly preprocessed. Three basic issues had to be solved:

- Reflections from background.
- Gap time during the image readout.
- Missing time synchronization with the global trigger.

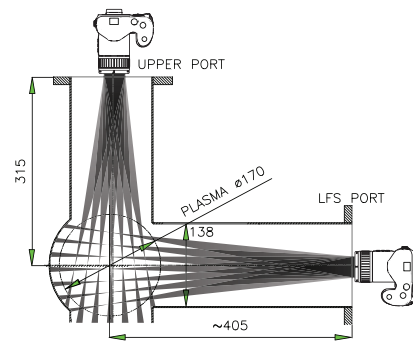


FIG. 3. Experimental setup for tomographic reconstruction: two cameras were placed perpendicular to each other.

The spatial profile of plasma light reflected from the tokamak chamber is strongly non-uniform as can be seen in the top image of Fig. 4. Increase of the camera signal at the beginning and end of each frame is caused by the fact that reflectivity of tokamak chamber segments along the lines of sight tangential to the port edges is significantly stronger compared to the section viewed by the central lines of sight. We employed singular value decomposition ($U\Sigma V^* = A$) to remove these artifacts in the signal due to non-homogeneous reflections. Each column of the decomposed matrix A corresponds to one image frame. Matrix U contains the spatial (*topos*) and matrix V temporal (*chronos*) singular vectors. After the decomposition, any time evolution is removed from the first two *topos* vectors and also these two vectors are smoothed in the spatial direction. The projection of these vectors is subtracted from the original image and the resulting set of images is once more decomposed. This time, the first SVD vectors contain a majority of the reflection patterns, and therefore, the first few vectors are smoothed and the original image is recovered.

In the second step, the missing gaps have to be calculated. Therefore, the images are once more decomposed using the SVD. However, this time the vectors of the decomposed matrix are columns of each image. The *topos* vectors and their time evolutions given by *chronos* vectors are obtained from the SVD. The fast Fourier transformation for incomplete data⁵

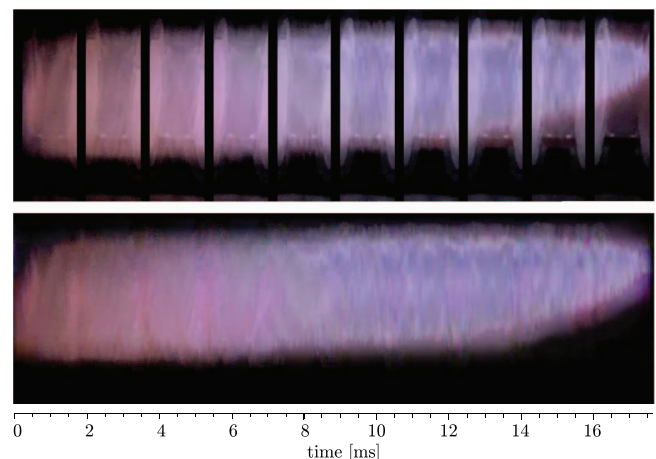


FIG. 4. An example of original (top) and preprocessed (bottom) image sequence from discharge #7251 (discharge in helium) obtained by the LFS camera (Fig. 3). The image is in real color.

is used to interpolate the quazi-periodic chronos in the missing gaps. The Fourier transformation is applied on 0.1 ms windows around each gap and then the ordinary inverse Fourier transformation is computed and the missing time evolution is estimated. The gaps have to be filled in order to increase the number of time slices suitable for the reconstruction by up to 34% in the case of the two cameras.

Finally, it is necessary to synchronize the video from the cameras with the global timing during postprocessing. In our case, we have successfully tested a high power flash with a very short pulse as the synchronization element.

III. EXAMPLE OF RESULTS

A. Plasma images and emissivity reconstruction

The main task of plasma tomography is reconstruction of plasma emissivity. Because it is an ill posed and under-determined problem, some *a priori* knowledge must be assumed:

1. Plasma toroidal symmetry – to use the rolling shutter effect because the camera samples a different region of the plasma.
2. Smooth emissivity profile – the optimal solution minimizes the Fisher information with the measurements as constraints.⁶
3. Boundary conditions – zero emissivity is assumed out of the scrape-of-layer and only positive emissivity inside.
4. Spatial frequency of the plasma emissivity in the radial direction is higher than in the poloidal direction. Therefore, smoothness is preferred along the flux surfaces. However, an iterative self-consistent approach is applied in order to find the emissivity centre because the plasma position in the GOLEM tokamak is not known precisely.
5. Furthermore, the divergence of the chords (lines-of-sight) is not negligible. It is important to consider that these chords form cones with vertex in the focal plane (see Fig. 3). Each real chord is replaced by an approximating set of “virtual” line chords.

Thanks to high universality, the pixel based algorithms are the most appropriate for our purposes. An algorithm minimizing the Fisher information⁶ is used. The speed and memory usage of this algorithm is greatly improved⁷ to allow reconstruction of hundreds of chords as well as a high resolution of the reconstruction. The high spatial resolution is necessary in order to minimize Moiré artifacts caused by 336 chords from each of the camera.

Using the corrected output from both cameras, tomographic reconstruction was performed. The reconstructed emissivity for discharge #7251 at 11.1 ms is plotted in Fig. 5. The observed profile was flat or shallowly hollow. This profile was probably caused by an influx of neutrals from the tokamak wall. Neutral particles penetrate through the plasma because the mean free path of neutrals is comparable with the plasma diameter.

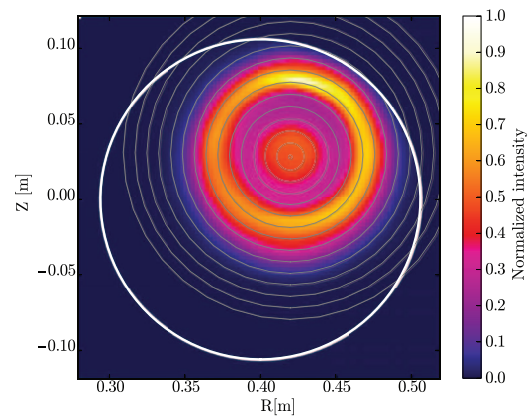


FIG. 5. An example of the tomographic reconstruction for discharge #7251 at 11.1 ms. Only the red component is plotted. Gray lines correspond to the expected magnetic field and the white line is the border determined by a limiter of the tokamak.

The reconstruction was used to determine the plasma position and correct integration drift of the magnetic sensors used as standard diagnostics for position estimation. The disadvantage of the flatness of the emissivity is that it can lower the credibility and thus, increase uncertainty of the determined position.

IV. SUMMARY

Examples of usage of the cheap high speed camera EX-F1 have been presented in this paper. First, tomographic reconstruction with all necessary corrections – linearity, background subtraction, and advanced gaps filling was done. Moreover, advanced tomographic reconstruction based on minimization of Fisher information with a customized smoothing matrix has also been successfully performed. The results are optimistic and suggest that this camera could be considered as a low cost, versatile diagnostic for small tokamak experiments.

ACKNOWLEDGMENTS

This work was supported by the Grant Agency of the Czech Technical University in Prague, Grant No. GS11/131/OHK4/2T/14.

¹M. A. Zeeland, J. H. Yu, N. H. Brooks, W. W. Heidbrink, K. H. Burrell *et al.*, *Plasma Phys. Controlled Fusion* **52**, 045006 (2010).

²S. Yoshihara, Y. Nitta, M. Kikuchi *et al.*, *IEEE J. Solid-State Circuits* **41**, 2998 (2006).

³J. Gu, Y. Hitomi, T. Mitsunaga, and S. Nayar, *IEEE International Conference on Computational Photography* (2010), pp. 1–8.

⁴V. Svoboda, J. Mlynar, G. Pokol, J. Stockel, and G. Vondrasek, *Fusion Eng. Des.* **86**, 1310 (2011).

⁵V. Y. Liepin'sh, *Autom. Control Comput. Sci.* **30**, 20 (1996).

⁶M. Anton *et al.*, *Plasma Phys. Controlled Fusion* **38**, 1849 (1996).

⁷M. Odstrcil, J. Mlynar, T. Odstrcil, B. Alper, A. Murari, and JET EFDA Contributors, “Modern numerical methods for plasma tomography optimisation,” *Nucl. Instrum. Methods Phys. Res. A* (in press).